Check for updates

Formaldehyde-free melamine microcapsules as core/shell delivery systems for encapsulation of volatile active ingredients†

G. León, N. Paret, P. Fankhauser, D. Grenno, P. Erni, L. Ouali and D. L. Berthier [ID] *

The release of volatile bioactive molecules, such as fragrances, can be controlled by microencapsulation in core–shell polymeric delivery systems. Currently, most of the available polymers are based on melamine–formaldehyde materials, and the release is generally triggered by the rupture of the brittle and stiff shell. However, formaldehyde-based chemistry may often be undesirable in applications for consumer goods such as personal care products or detergents for fabrics, and there is a strong need for formaldehyde-free microcapsules in these applications. In this article, formaldehyde is successfully substituted by glyoxal and its derivatives to allow the polymerization of melamine and other amines to prepare oligomers as starting point for core/shell polymerization. The oligomer synthesis is optimized *via* the reactant composition and towards an enhanced potential cross-linking density. The formulations with the most branched oligomers are applied at the interface of oil-in-water emulsions to prepare microcapsules. Their capacity to retain volatile molecules is measured by thermogravimetry and their mechanical properties are measured by micromechanical testing using compression–retraction cycles on multiple individual microcapsules. The results reveal an excellent retention capacity for volatile molecules and tunable mechanical properties that make these capsules highly suitable as a formaldehyde-free alternative to conventional aminoplast microcapsules.

1. Introduction

Delivery systems for the controlled release of bioactive molecules are of growing interest not only in industry but also in academia.[1–5] Physical or chemical delivery systems have been developed to control the release of these molecules as a function of time or to improve their deposition on various surfaces.[6,7] Among the different physical delivery systems, core–shell microcapsules are among the most developed ones not only to control and extend the release of bioactive molecules, but also to protect them against degradation.[8] Microencapsulation typically consists of the preparation of an emulsion followed by the formation of a polymer shell by interfacial or induced phase-separation polymerization, resulting in core–shell structures.[9] Release can be obtained by the rupture of the shell by various stimuli.[10–12] For example, release of the encapsulated load can be triggered mechanically by rubbing the capsules trapped on a surface,[13,14] by a raise of the temperature[10,15] or upon irradiation with light.[16,17] Microcapsules are nowadays present in many applications including self-healing

composites,[18] ink for carbonless copy paper,[19] agrochemicals[20] or volatile perfume molecules.[7,21,22]

Shell materials suitable for the encapsulation of small-molecular weight molecules are typically polymers such as polyamide,[23] polyurea,[24–26] polyurethane[9] and urea/melamine–formaldehyde.[7,12,13,21] Due to the low cost and the ready availability of the starting materials, to the high yield of encapsulation, and to the mechanical properties of the resulting polymer shells, urea or melamine–formaldehyde microcapsules obtained from aminoplast resins have been developed in various applications, including home care consumer goods.[7] These resins are usually polymerized to form the shell under acidic conditions.[27,28] The high valency of melamine leads to highly cross-linked barrier materials at the oil–water interface.[13]

The main drawback of melamine–formaldehyde resins and capsules is the capability of these materials to release formaldehyde.[29] The addition of amines on formaldehyde is reversible under acidic conditions. The resulting polymers may contain unreacted formaldehyde, or can degrade and release it during storage. Lam *et al.* have reported that if formaldehyde is not metabolized, it can cross-link between proteins and DNA.[30] In view of related safety concerns, the US Environmental Protection Agency has established a maximum daily dose reference of 0.2 mg kg^{-1} body weight per day for formaldehyde.[31–33] There is therefore an increasing demand to reduce or remove it from existing aminoplast delivery systems.[34,35] Microcapsules with

low formaldehyde content have been obtained by changing the temperature of the process[36] or the addition of various scavengers such as ammonia,[36] ethylene urea[37] or resorcinol.[7,36,37] Alternatively, Li and coworkers prepared microcapsules with aminoplast resins having a lower formaldehyde–melamine molar ratio than conventional copolymers.[36] Microencapsulation properties were reported to be unchanged with these low formaldehyde-content resins.[38] Nonetheless, a complete removal has not yet been reported. As a consequence, alternatives to aminoplast microcapsules have been investigated with polyurea, polyamide or coacervate shell materials.[9,23–25,30] Despite the absence of formaldehyde, the properties of these microcapsules were not as performing as those of aminoplast microcapsules, with soft shells difficult to break upon rubbing.[12,21] Indeed, the presence of a melamine–formaldehyde shell affords very good release properties.[21] In this context, formaldehyde-free melamine copolymers have previously been investigated to prepare microcapsules.[29] Despres et al. reported the preparation of urea or melamine prepolymers with 2,2-dimethoxyethanal (DME) as a non-volatile substitute of formaldehyde.[39] They described the mechanism of the polymerization between melamine and DME. Nevertheless, a low conversion was obtained and only dimers of melamine were observed. The equivalent resin prepared with urea was nonetheless successfully used to prepare binders for wood composite boards.[40] Our overview suggests that while several approaches have been described to form aminoplast polymers with reduced formaldehyde content, a consistent synthesis route to build robust, formaldehyde-free microcapsules for the delivery of small molecular weight bioactive molecules remains elusive. The synthesis of formaldehyde-free aminoplast capsules with controlled mechanical properties and high encapsulation efficiency remains a considerable challenge, which we will address herein.

In the present study, our objective was to prepare formaldehyde-free aminoplast resins and to evaluate their suitability as barrier materials for robust and stable core/shell capsules for volatile molecules, in particular to encapsulate volatile fragrance compounds. Our approach is based on using dialdehydes, and in particular glyoxal, a precursor of DME to obtain formaldehyde-free polymer shells for efficient microencapsulation. Resins based on glyoxal were prepared with different amines, including melamine and urea. Liquid chromatography with Time-Of-Flight (TOF) detection was used to obtain a qualitative analysis of the resin during the polymerization. This approach allowed to afford not only a good understanding of the formation mechanism of the resin, but also to detect suitable oligomers to create a cross-linked polymer shell. Based on this evaluation, optimized resins in terms of synthesis conditions and compositions were used to prepare core/shell microcapsules. To form these capsules, the active ingredient (here: a model mixture of five fragrance compounds) was emulsified into the aqueous phase, and the capsule shells were formed by a combination of resin deposition at the oil/water interface and additional *in situ* crosslinking. Finally, the resulting capsules were analyzed in terms of their mechanical properties to determine if the substitution of formaldehyde by

glyoxal and 2,2-dimethoxyethanal in melamine capsules lead to delivery systems with a performance in terms of volatile molecule release comparable to traditional capsules.

2. Results and discussion

2.1. Preparation of formaldehyde-free melamine resins

2.1.1. Methodology for oligomer analysis: example of melamine and 2,2-dimethoxyethanal in copolymer 3. Melamine can react with aldehydes to give aminoplast copolymers.[27,28] In the presence of 2,2-dimethoxyacetaldehyde (DME or **1**, Fig. 1), this polymerization can be controlled by the pH as observed with formaldehyde.[39,40] Under basic conditions, the addition of the amino group on the aldehyde formed amino-alcohol **2a** (Fig. 1). In the presence of a monoaldehyde, the polymerization cannot occur by polyaddition. The polymerization is usually initiated by the addition of an acid catalyst.[27] Under acidic conditions, the amino-alcohol **2a** loses a molecule of water and generates an imine (**2b**). The addition of the amino group of melamine or **2a** on the imine is the first step of this polycondensation to afford polymer **3** (Fig. 1).

The high valency of melamine can lead to the formation of a large number of various oligomers. Different techniques have been used to characterize aminoplast resins.[27,39] Steinhof et al. described the use of ^{15}N-NMR to determine the mechanism of urea–formaldehyde polymerization.[41] More recently, Lavric reported the accurate mass determination of melamine–formaldehyde resins by HPLC-MS with two ionization techniques, electrospray ionization (ESI) and atmospheric pressure chemical ionization (APCI) with a source temperature of 350 °C.[42] In the present work, a high resolution LC/ESI-TOF-MS system was used to characterize our oligomers. The detection *m/z* window was in the scan range from 103 to 3000 with a source temperature at 325 °C. This temperature was controlled to prevent possible reactions in the source and was in the same range than those reported with melamine resins.[42]

As a model reaction, melamine and three equivalents of DME were dispersed in water at pH 9.5. The reaction mixture was warmed-up to 60 °C for 30 min to give a solution. Then, nitric acid was added to reach a pH of 4.5 to initiate the polymerization and the temperature was maintained at 60 °C for 2 h. An aliquot of the solution was then analyzed by LC/ESI-TOF-MS as described above (Table 1). Several peaks were observed in
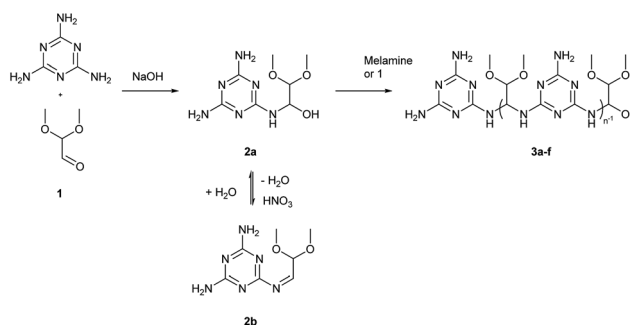

Fig. 1 Structure of linear poly(melamine-*co*-2,2-dimethoxyethanal) **3**.

Table 1 Mass-to-charge ratio m/z found and calculated with a high resolution by LC/ESI-TOF-MS, affording the corresponding formula of oligomers in copolymer **3** prepared with melamine and DME

m/z [M + H]$^+$ (found)	m/z (calcd)	$\Delta m/z$ (ppm)	Formula	Compounds	n
443.22483	443.22219	5.96	$C_{14}H_{26}N_{12}O_5$	**3a**	2
551.28031	551.27702	5.98	$C_{17}H_{30}N_{18}O_4$	**3b**	3
763.38181	763.37919	6.05	$C_{24}H_{42}N_{24}O_6$	**3c**	4
1061.51935	1061.51814	1.14	$C_{35}H_{60}N_{30}O_{10}$	**3d**	5
1187.58647	1187.58354	2.47	$C_{38}H_{66}N_{36}O_{10}$	**3e**	6

the analysis corresponding to different oligomers of copolymer **3**. The high resolution of the TOF-MS detector allowed the determination of chemical formula from the comparison between calculated and measured molecular weights, represented by $\Delta m/z$ in ppm (Table 1). A formula is confirmed when $\Delta m/z$ is lower than 20 ppm. As a consequence, it was possible to calculate the exact masses of different oligomers of melamine and DME and to compare them with the measurements from the reaction mixture of copolymer **3** to identify possible structures (Table 1).

Different chemical formulae were deducted from the measurements with deviations below the limit of 20 ppm for oligomers from dimers **3a** with m/z at 443.22483 g mol^{-1} to hexamer **3e** with m/z at 1187.58647 g mol^{-1} (Table 1). We observed that in oligomers of **3** detected by TOF-MS, only one equivalent of DME was grafted on the melamine, corresponding to a repeating unit based on molecules **2a** or **2b**. The LC/ESI-TOF-MS allowed not only a good interpretation of the mechanism of polymerization between melamine and DME but also showed that DME cannot be used to cross-link melamine under acidic conditions in contrast to formaldehyde. As a consequence, and because crosslinking is a mandatory step to obtain performing microcapsules, reactions between melamine and other amines with glyoxal (GY), a dialdehyde, were investigated with this technique.

2.1.2. Preparation of copolymers 4 of glyoxal and melamine. Melamine and three equivalents of glyoxal were dispersed in water as described above. Under basic conditions, a fast polymerization occurred and a gel was obtained. The presence of dialdehyde with a triamine obviously led to a cross-linked material by polyaddition. Only a large excess of glyoxal (6 eq. min) gave a stable solution. The same reaction was carried out at pH 5.0 and stable solutions were obtained. Thus, the reaction mixture was analyzed by LC/ESI-TOF-MS. Despite the different conditions of pH, temperature and time, only dimers of

melamine were obtained. The highest reported m/z in each mixture varied from 275.12 to 427.15 (Table 2). The proposed structures of these dimers are reported in Fig. 2. The addition of two melamine molecules on glyoxal can give products **4a** or **4a′** with a m/z of 293.13. The presence of dimer **4b**, which does not contain any oxygen atom, suggests that dimer **4a** is the major product. In addition, we suppose that dimer **4a** is in equilibrium with dimer **4c** in a keto–enol tautomerism-like equilibrium. This latter dimer looks to be more stable than **4a**. Because of the high dilution of the samples, it was not possible to obtain a good signal in NMR to determine the exact structure of the dimer **4a**, **4a′** and **4c**. All structures are supposed to be present in the solution. Nonetheless, ^{1}H-NMR spectra of formaldehyde, GY, and DME, were recorded in water. The results showed that these aldehydes were present as hydrates and for formaldehyde and glyoxal, as dimers (Table 3). As a consequence, the presence of hydrated aldehyde groups in dimers **4d** and **4e** suggests that the probability to have dimer **4a′** is low.

Despite the fast polymerization under basic conditions, only dimers were obtained by polycondensation. The lower reactivity of GY, compared with that of DME, probably due to the presence of a second aldehyde group and the steric hindrance of melamine, highlighted in dimer **4a′**, may explain the low reactivity and the limited conversion. The presence of less hindered or more nucleophilic amino groups may lead to higher conversion with GY.

2.1.3. Preparation of copolymers 6 with glyoxal and urea. Melamine was substituted by urea, also used as comonomer with formaldehyde in aminoplast resin. Despite the lower reactivity of the urea NH$_2$ group, urea can easily react with formaldehyde to afford microcapsules. According to the protocol described above, urea was dissolved in water with one equivalent of glyoxal at pH 6 or in the presence of sodium hydroxide at pH 9. The reaction was carried out at 60 °C for different periods of time, from 0.5 to 4 h. The structures of

Table 2 Mass-to-charge ratio m/z found as a function of reaction conditions and chemical structures of dimers **4** from the reaction of glyoxal and melamine

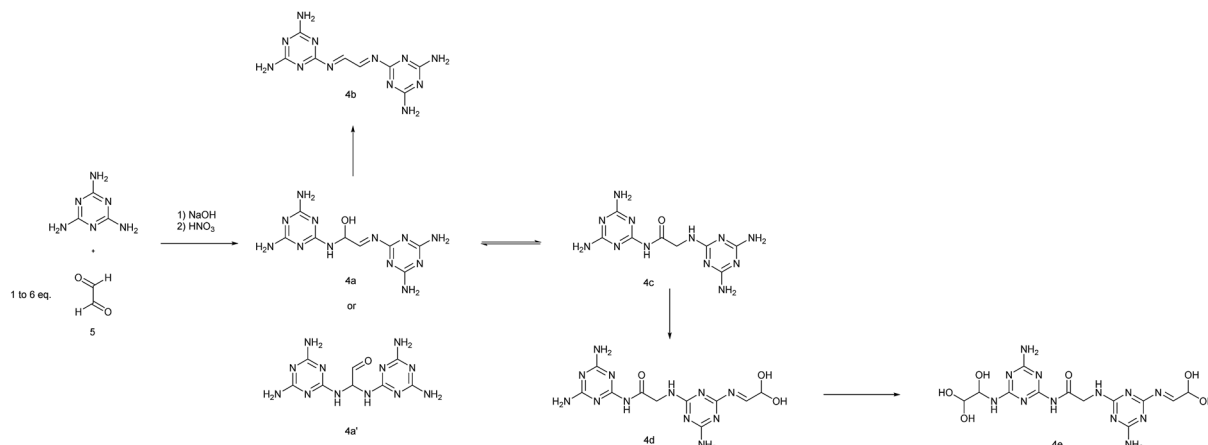| M/GY (eq.)	pH	Time (h)	T (°C)	m/z [M + H]$^+$ (found)	$\Delta m/z$	Formula	Compounds
1/3	9	0.1	60	—		Precipitate	**4**
1/1.5	5	2.5	60	293.13043	14.7	$C_8H_{12}N_{12}O$	**4a, 4a′** or **4c**
1/1.5	4	1	60	351.13527	15.1	$C_{10}H_{14}N_{12}O_3$	**4d**
1/1.5	4.5	0.1	80	427.15690	16.2	$C_{12}H_{18}N_{12}O_6$	**4e**
1/6	4.8	3	60/90	275.12287	10.5	$C_8H_{10}N_{12}$	**4b**

Fig. 2 Proposed structures of oligomers present in copolymer **4** from the polymerization of melamine and glyoxal observed by LC/ESI-TOF-MS.

Table 3 Structures and concentrations of formaldehyde, 2,2-dimethoxyethanal, and glyoxal in water by ^{1}H-NMR in D_2O

Aldehydes	Structures observed by ^{1}H-NMR				
Formaldehyde 37% aq.	< 1%	72%	12%	12%	4%
DME (**1**) 60% aq.	< 1%	< 1%	> 99%		0%
Glyoxal (**5**) 40% aq.	< 1%	< 1%	> 98%		0%

oligomers were resolved by LC/ESI-TOF-MS (Table 4). Under these conditions, as observed with melamine, only dimers were obtained with m/z from 143.05 to 317.07 with compounds having the proposed structures **6a** and **6d** (Fig. 3). These conditions did not favor the addition of NH_2 group of urea on imine groups of proposed products **6c** or **6d**. In contrast, in the

presence of nitric or formic acid as catalyst and an excess of urea with respect to the glyoxal (two or four equivalents), polycondensation started with the formation of trimers **6e**, tetramers **6f**, **6g** and **6h**, and even pentamers **6i**. This polymerization can be linear as observed in **6f** or branched in compounds **6g** and **6i**. Surprisingly, the presence of aldehyde groups, probably

Table 4 Mass-to-charge ratio m/z found by LC/ESI-TOF-MS during the copolymerization of urea and glyoxal and proposed chemical formula of oligomers **6a–i**

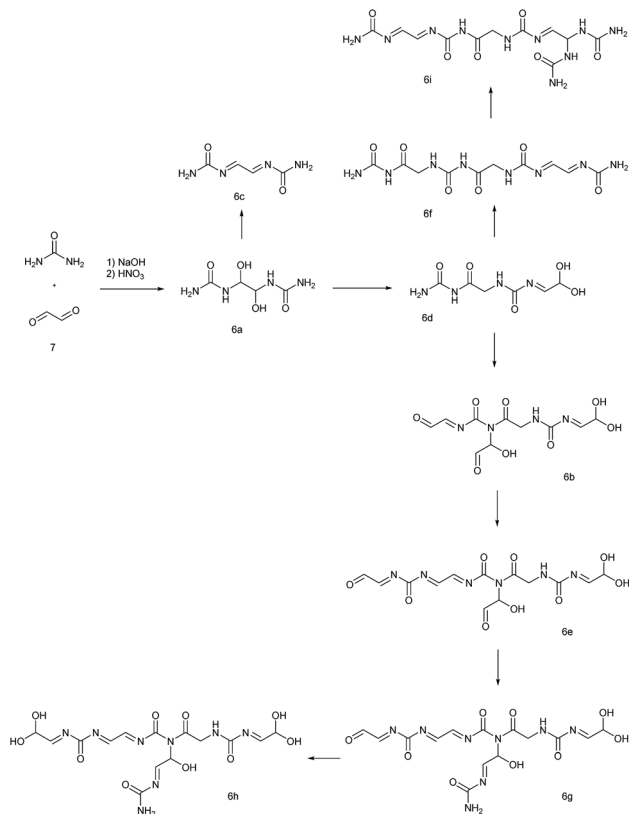| U/GY molar ratio	pH	Time (h)	T (°C)	m/z [M + H]$^+$ (found)	m/z (calcd)	$\Delta m/z$	Formula	Compounds
1	9.4	0.5	60	179.08148	179.078031	−19.2	$C_4H_{10}N_4O_4$	**6a**
				143.05843	143.056901	−10.7	$C_4H_6N_4O_2$	**6c**
1	6	3	60	317.06933	317.073341	12.6	$C_{10}H_{12}N_4O_8$	**6b**
				219.07114	219.072946	8.2	$C_6H_{10}N_4O_5$	**6d**
2	9/4.6	1/1	80	399.09191	399.090054	−4.7	$C_{13}H_{14}N_6O_9$	**6e**
				343.10630	343.111457	15.0	$C_{10}H_{14}N_8O_6$	**6f**
				441.10789	441.111852	9.0	$C_{14}H_{16}N_8O_9$	**6g**
				459.11686	459.122417	12.1	$C_{14}H_{18}N_8O_{10}$	**6h**
4	8.8/4.5	0.5/6	80	385.12726	385.133255	15.6	$C_{11}H_{16}N_{10}O_6$	**6i**

Fig. 3 Proposed structures of oligomers **6a–i** from the copolymerization of urea and glyoxal according to the LC/ESI-TOF-MS measurements.

Table 5 Mass-to-charge ratio m/z found by LC/ESI-TOF-MS during the copolymerization of guanazole and glyoxal and proposed chemical formula of oligomers **7a–i**

m/z [M + H]$^+$ (found)	m/z (calcd)	$\Delta m/z$ (ppm)	Formula	Compounds
158.06701	158.067800	5.0	$C_4H_7N_5O_2$	**7a**
239.11098	239.11173	3.1	$C_6H_{10}N_{10}O$	**7b**
297.11799	297.117210	−2.6	$C_8H_{12}N_{10}O_3$	**7c**
378.16193	378.161140	−2.1	$C_{10}H_{15}N_{15}O_2$	**7d**
320.160	320.15566	−13.6	$C_8H_{13}N_{15}$	**7e**
459.20425	459.205070	1.8	$C_{12}H_{18}N_{20}O$	**7f**
540.24548	540.249	6.5	$C_{14}H_{21}N_{25}$	**7g**
696.25154	696.254875	4.9	$C_{20}H_{25}N_{25}O_5$	**7h**
777.29674	777.298805	2.7	$C_{22}H_{28}N_{30}O_4$	**7j**
858.33620	858.342735	7.6	$C_{24}H_{31}N_{35}O_3$	**7k**
939.39880	939.386665	−12.9	$C_{26}H_{34}N_{40}O_2$	**7i**

a lower molar ratio between guanazole and glyoxal, suggesting a fast polymerization. The reaction mixture was then analyzed as described above (Table 5). Linear oligomers **7a–d** were observed and structures were proposed based on the polyaddition mechanism (Fig. 5). Dimers **7b** and trimmers **7c** of guanazole were detected with m/z at 297.12 and 378.16, respectively. The conversion of the polymerization was monitored by LC/ESI-TOF-MS analyses and the presence of trimers **7e** was detected after 45 min. Larger oligomers then appeared with branched tetramers and pentamers **7f** and **7g** after 2.5 h. The latter, similarly to trimmer **7e**, has a chemical formula obtained by MS which contains only C, H and N (Table 5). According to this formula, two structures can be drawn, one with two triple additions of guanazole on glyoxal (**7g**, Fig. 5) or another with one double addition and one tetra-addition (**7g′**, see Fig. S1 in ESI†). Because of the steric hindrance of guanazole compared with urea, a tetra-addition is not likely to be observed. Then, we observed that compound **7g** reacted with glyoxal and guanazole to afford pentamers with proposed structures **7h** and also octamers **7i**, via hexamer and heptamer **7j** and **7k**, not represented in Fig. 5 (m/z in Table 5). We assume that a better water solubility and a slightly lower pK_a increased the conversion of the polymerization of guanazole with glyoxal.

due to the low pH of the reaction mixture, was suggested in structures **6b**, **6e** and **6g**. The latter seems to be in equilibrium with **6h**. It is also important to note that the highest degrees of polymerization were obtained at 80 °C, suggesting that the conversion is temperature-dependent. As a consequence, despite the lower reactivity of NH$_2$ groups from urea, its lower steric hindrance seems to allow longer polymer chains.

2.1.4. Preparation of copolymers 7 with glyoxal and guanazole. The second amine tested to replace melamine is the 1*H*-1,2,4-triazole-3,5-diamine, known as guanazole (GZ or **8**). This compound, as for melamine, is a reaction product of cyanamide and is readily soluble in water up to 15 wt%. Guanazole has a tautomeric equilibrium and H-bonding capability (Fig. 4). It has a similar basicity as melamine with pK_a at 4.43 and 5.00, respectively.[43,44] Protonation of guanazole normally occurs at the N-4 position and not on the NH$_2$ groups.

Guanazole was dissolved in water and mixed with glyoxal at pH 8 and 60 °C to favor the polyaddition. A large excess of amine (10 eq.) was used to prevent the precipitation of the copolymer **7**. Indeed, precipitation occurred rapidly with

2.1.5. Preparation of formaldehyde-free aminoplast copolymers 9. Polymerization of melamine with DME or glyoxal did not lead to cross-linked polymers or branched structures in contrast to those of urea or guanazole. The latter is more reactive than urea and its polymerization with glyoxal was difficult to control. Furthermore, the steric hindrance of DME compared with that of glyoxal (Table 1), may limit the formation of desired branched oligomers despite its higher reactivity with melamine. Thus, urea and melamine were copolymerized in the presence of glyoxal and DME to afford formaldehyde-free aminoplast copolymers **9** with possible branched oligomers. The reactions were carried out under acidic conditions at 60 °C with melamine/urea and glyoxal/DME molar ratios of 1 and 2, respectively. The total NH$_2$/CHO molar ratio was fixed at 1. In a second experiment, melamine and an excess of urea were

Fig. 4 Chemical structure of guanazole **8** and one of its tautomers.
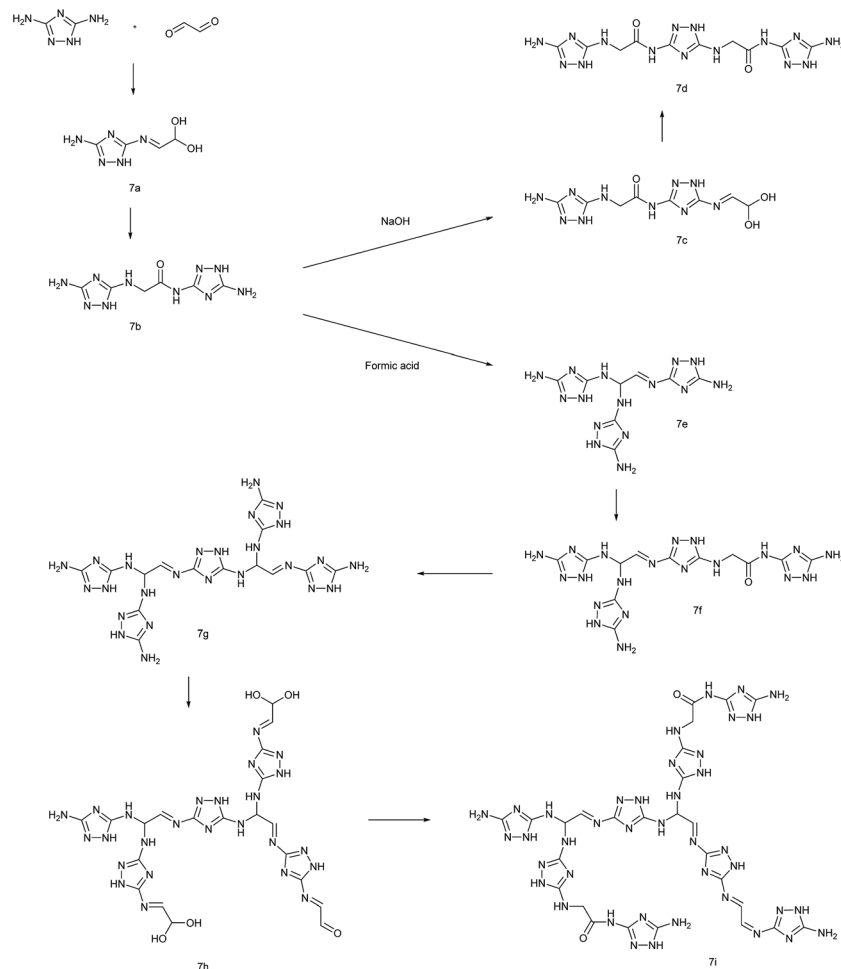
Fig. 5 Proposed structures of oligomers **7a–i** from the copolymerization of guanazole and glyoxal according to the LC/ESI-TOF-MS measurements.

Table 6 Exact masses and proposed chemical formula of branched oligomers in copolymer **9**. Reaction time was 4 h

U/M	T (°C)	m/z [M + H]$^+$ (found)	$\Delta m/z$ (ppm)	Formula	Compounds
1	60	395.19043	8.32	$C_{10}H_{18}N_{16}O_2$	**9a**
3	80	401.18557	−5.58	$C_{11}H_{16}N_{18}$	**9b**
		571.22405	−11.22	$C_{15}H_{26}N_{18}O_7$	**9c**

copolymerized with glyoxal at 80 °C. Melamine/urea and NH$_2$/CHO molar ratios were fixed at 3 and 4.5, respectively. The reaction products were then qualitatively analyzed by LC/ESI-TOF-MS (Table 6).

At 60 °C, urea reacted with melamine and glyoxal to give the product **9a**. According to the formula obtained from the MS analysis and the starting materials of the reaction, only structure **9a** proposed in Fig. 1 can be obtained. It confirmed that two equivalents of melamine and two others of less hindered urea can be added on one molecule of glyoxal, affording a dense cross-linking. At 80 °C and with an excess of amino groups, it was possible to graft three molecules of melamine onto one molecule of glyoxal with product **9b** (Fig. 6). Based on its analysis, only the proposed structure **9b** can be formed. Under these

conditions, we can expect a cross-linking of the melamine with the glyoxal. A second branched oligomer, with structure **9c**, was obtained at 80 °C, mixing grafted urea and linear melamine repeating units (Fig. 6). As a consequence, the combination of melamine with urea in the presence of glyoxal and DME can lead to the preparation of branched polyamines, key ingredients in the preparation of formaldehyde-free microcapsules.

2.2. Formation of formaldehyde-free melamine microcapsules for volatile delivery: encapsulation of model fragrance compounds

2.2.1. No additional cross-linking. We have observed above by LC/ESI-TOF-MS (Fig. 6) that the presence of glyoxal is
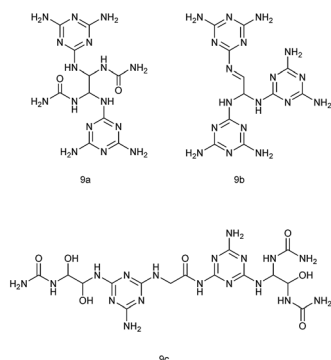
Fig. 6 Proposed structures of oligomers **9a–c** present in formaldehyde-free aminoplast resins.

necessary to obtain a good cross-linking between amines and aldehydes whereas the presence of DME gives good conversion to the resins. The composition of the copolymer **9** is crucial to stabilize not only the oil-in-water emulsion necessary to prepare the microcapsules, but also to afford an efficient capsule shell for the volatile retention. Capsules **A–D** were thus prepared with different compositions based on copolymer **9** with various glyoxal/DME molar ratios from 2 (**A**) to 10 (**D**) and a urea/melamine (U/M) molar ratio of 3 (Table 7). According to the previous LC/ESI-TOF-MS analyses we can expect that the

copolymer of the shell should have similar oligomers but with probably different compositions.

Capsules were obtained from an oil-in-water emulsion of a mixture of volatile fragrant molecules in water. The emulsion was stabilized in the presence of Ambergum 1221, a low M_w carboxymethyl cellulose and resins **A9–D9**, which were mixed together in water to give a solution. The oil phase was then added and the emulsion was prepared under high shear with a rotor/stator mixer. Then, an aqueous solution of Alcapsol 144, a copolymer of acrylic acid and acrylamide, was added to prevent droplet coalescence in the emulsion. This copolymer is commonly added to melamine–formaldehyde microcapsules as colloidal stabilizer.[21] The pH value of the solution was slightly acidic to initiate the polymerization of **9**, it was then maintained at 5.4 to keep the copolymers anionic. The emulsion was warmed up to 75 °C for 3 h to foster the cross-linking of melamine and urea with glyoxal as observed above. Stable dispersions of capsules were obtained and characterized by light microscopy. The size of the capsules **A–D** was measured by flow particle imaging analysis and the value of their mean diameters varied from 16 to 33 μm. The variations of capsule size may be explained by the different compositions and physical properties of the resins but modest modifications of the interfacial tension with the perfume were observed (see Table S1 in ESI†). The size differences are probably influenced by the kinetics of resin

Table 7 Formaldehyde-free aminoplast core–shell microcapsules containing volatile fragrance compounds with membranes formed at different GY/DME molar ratios. Mean diameters are number-based averages obtained from flow particle imaging analysis (scale bar: 20 μm)

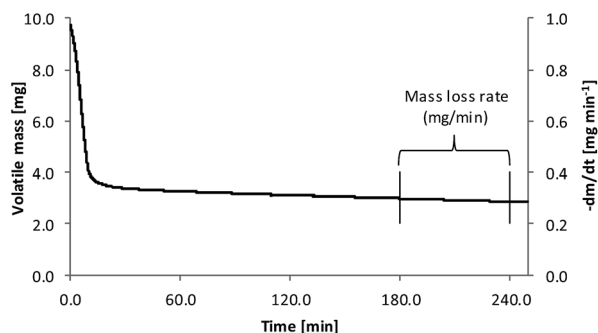| Microcapsule	GY/DME	D (μm)	Solid	Emulsion	Capsules
A	2	33	33.0		
B	4	16	35.2		
C	6	18	33.3		
D	10	33	37.1		

Fig. 7 Retention of encapsulated volatile molecules in microcapsule dispersion **B** (GY/DME molar ratio = 4; mean diameter: 16 μm) as measured by thermogravimetry at 50 °C as a function of time.
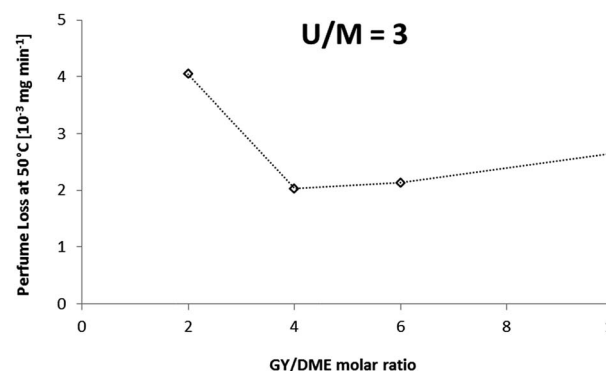

Fig. 8 Optimum glyoxal/DME molar ratio for retention of model volatile fragrance compounds in the core/shell microcapsules, as measured by TGA at 50 °C from microcapsules **A–D** at a constant urea/melamine molar ratio of 3. The most stable microcapsule is the one with the minimum volatile loss rate.

polymerization and its reaction with the carboxymethyl cellulose at the interface.

Then, the stability of capsules **A–D** was determined by assessing their hermeticity. The mass loss of encapsulated volatile molecules was measured by thermogravimetric analyses (TGA, Fig. 7). A droplet of the aqueous slurry was deposited in a crucible and its mass was measured as a function of time at 50 °C for 4.5 h. We observed that water was completely evaporated after about 25 min, resulting in a plateau corresponding to the solid content of the dispersion. With hermetic capsules, one would expect a perfectly flat plateau, suggesting the absence of leakage of volatile molecules from the capsule through the shell. We thus measured these rates of mass loss from the different capsules between three and four hours to compare the efficiency of the resins in terms of volatile retention (Table 8).

The results show that none of the capsules was completely hermetic (Fig. 8). Moderate leakages were observed from 4.04 to 2.03×10^{-3} mg min^{-1}. The capsules with the lowest leakage were those prepared with glyoxal/DME molar ratios at 4 and 6, corresponding to the capsules with the smallest mean diameters. This result is a discrepancy because usually the smaller the diameter of the capsule, the larger is the surface to cover and thinner is the shell.[17] We would expect that large capsules were the most stable with the thickest shells. In contrast, we suspect that the presence of a large shell can limit the conversion of the copolymerization and would not favor the cross-linking between oligomers because of the increase of the viscosity in the shell during the polymerization. As consequence,

compositions affording the smallest capsules were selected and their cross-linking improved to obtain hermetic capsules.

2.2.2. Additional cross-linking of microcapsules. Capsules were prepared as described previously for capsule **B** with a copolymer **9** having a NH$_2$/CHO molar ratio of 1. Concerning the cross-linking, on the one hand, a solution of urea or guanazole was added in the dispersion of capsules before the last step of the process to cross-link oligomers inside the shell. The dispersions with urea or guanazole were finally stirred at 75 °C for 1 h (capsules **B-U** and **B-GZ**, respectively in Table 9). On the other hand, hexamethylenediisocyanate (**10** or HDI, Fig. 9), used to prepare polyurea or polyurethane, was initially

Table 9 Effect of cross-linker choice and concentration on the stability of core/shell microcapsules containing volatile fragrance compounds. Microcapsule B was used for this comparison, and mass loss as a function of time at 50 °C was measured by TGA, with low mass loss rates of the volatiles indicating better stability of the microcapsule membrane

Microcapsules	Urea (%)	GZ (%)	HDI (%)	Volatile mass loss at 50 °C by TGA ($\times 10^{-3}$ mg min^{-1})
B-U-106	1.06			0.046
B-U-117	1.17			0.002
B-U-140	1.40			0.001
B-GZ-116		1.16		0.058
B-GZ-131		1.31		0.015
B-GZ-151		1.51		0.001
B-H-075			0.75	0.007
B-H-100			1.00	0.001
B-H-125			1.25	0.000

Table 8 Retention of encapsulated volatile molecules as a function of capsule compositions as monitored by thermogravimetry at 50 °C on microcapsules containing a mixture of five model fragrance compounds

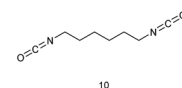| Microcapsules	Volatile mass loss at 50 °C by TGA (10^{-3} mg min^{-1})
A	4.043
B	2.029
C	2.129
D	2.656

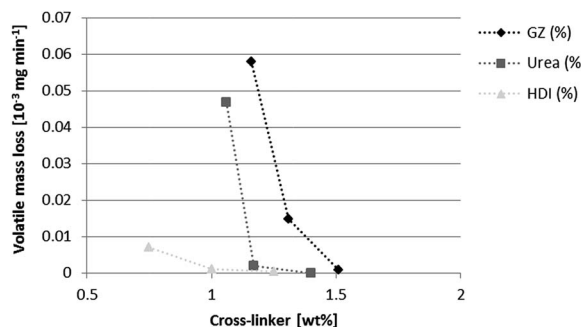Fig. 9 Structures of 1,6-hexamethylenediisocyanate (HDI) **10**.

Fig. 10 Stability of cross-linked microcapsule membranes for volatile encapsulation: volatile mass loss measured as a function of the concentration of the different cross-linkers added to the dispersion of microcapsules **B** and as a function of time at 50 °C by TGA.

dissolved in the oil phase to react with the amino groups of the copolymer **9** to cross-link the aminoplast shell (capsule **B-H**, Table 9).[35] The various cross-linkers were added at different concentrations and their influence on the mass loss of the capsules was measured as a function of time by TGA at 50 °C (Fig. 10). All capsules were obtained with a mean diameter comprised between 15 and 30 μm.

Urea was added at 1.06 wt% in the dispersion of capsules **B-U** (capsule **B-U-106**, Table 9) and their thermogravimetric analyses showed a significant decrease of the mass loss from 2.029 to 0.046×10^{-3} mg min^{-1}. Further addition of urea up to 1.40 wt% made the capsules **B-U-140** nearly hermetic with a loss at 0.001×10^{-3} mg min^{-1}. The same trend was observed with guanazole added instead of urea. The mass loss also decreased up to 0.001×10^{-3} mg min^{-1} during the last hour of measurement at 50 °C but a slightly higher concentration of guanazole was necessary at 1.51 wt% (capsule **B-GZ-151**, Table 9). These results confirm that an excess of amines, urea or guanazole, favors the cross-linking in the shell, as also observed in the neat resin. We assume that this reaction reduces the porosity in the capsule wall, limiting the possibility of diffusion of small-molecular weight volatile compounds, such as perfume ingredients, through the shell.

In the presence of HDI, the cross-linking reaction between the amino groups of the resin and the isocyanate functions should take place at the oil/water interface. At 0.75 wt% of HDI, mass loss decreased to 0.007×10^{-3} mg min^{-1}, which was very low compared with urea or guanazole. A completely flat plateau with no evaporation was observed with 1.25 wt% of HDI, affording a hermetic capsule **B-H-125** (Table 9). The presence of a polyurea shell at this interface seems to improve the volatile retention as observed by TGA (Fig. 10).

2.3. Mechanical behavior of microcapsules for release controlled by shell rupture

The typical release mechanism for volatile molecules released from the core/shell capsules synthesized here in applications occurs by mechanical cleavage of the shell upon rubbing.[21,22,45] Substitution of traditional melamine–formaldehyde resins by our oligomers is expected to influence the mechanical properties of the capsules.

To assess the role of the different capsule shell chemistries for the mechanical properties of the capsules, microcapsules were prepared from copolymer **9** (having a NH$_2$/CHO molar ratio of 1) with additional cross-linking, as described above. We thus measured force–deformation curves of the formaldehyde-free capsules described in the present article and compared them with those of classical melamine–formaldehyde micro-capsules. For this part of the study, the following capsules were selected to study the role of different monomer compositions and synthesis conditions for the mechanical properties: **B-U-140** (additional cross-linking of the shell using urea in the aqueous phase), **B-GZ-151** (cross-linking using guanazole in the aqueous phase) and **B-H-125** (cross-linking using HDI in the oil phase).

We investigated the mechanical properties at large defor-mations far outside the linear regime to break the capsules, as is the case under typical application conditions. Using a micro-mechanical testing device, we performed compression–retrac-tion cycles on multiple individual microcapsules within each sample, and we compared the resulting force *vs.* displacement curves for the three different shell types. Fig. 11 shows a comparison of force–deformation curves measured on a clas-sical melamine/formaldehyde-based microcapsule with two different formaldehyde-free microcapsules: cross-linked gua-nazole in the aqueous phase, and HDI initially added to the oil phase. Intermediate maxima in the force curves are interpreted as capsule rupture events (cases a and c in Fig. 11, with the peak force indicated by the star symbols), whereas capsules without sudden rupture reveal monotonically increasing force curves (case b in Fig. 11, with the peak force simply corresponding to the end of the approach measurement). All curves reveal significant hysteresis between the approach and retract steps, meaning that in all cases the compression of the capsules is predominantly irreversible: once compressed, they do not rebound to their original size. This is the case even for capsules without a clear rupture event (case b), indicating that the encapsulated oil is lost gradually *via* slow expulsion, rather than by a sudden fracture. For the urea-only formulation (data not shown), the resulting capsules were unstable at the conditions of this measurement and no characteristic mechanical response could be observed. In contrast, if guanazole was added to the water phase the capsules exhibited more robust mechanical behavior, but did not reveal the typical peaks or plateaus associated with mechanical rupture. For capsules with HDI added to the oil phase initially, the mechanical measure-ments reveal an interesting combination of robustness and breakability: the capsules are stable and remain intact until the force measurement is performed, but they can be made to rupture under relatively moderate forces revealing character-istic burst peaks and significant release of liquid (as shown by the negative force values measured during retraction, indicating that the released liquid adheres to the surface of the force sensor). Previous investigations have focused on the linear deformation regime at small deformations to obtain material properties of classical, intact melamine capsule shells.[21] Fig. 6 also summarizes the peak force values plotted against the cor-responding deformation values γ_{peak} (the deformation at which
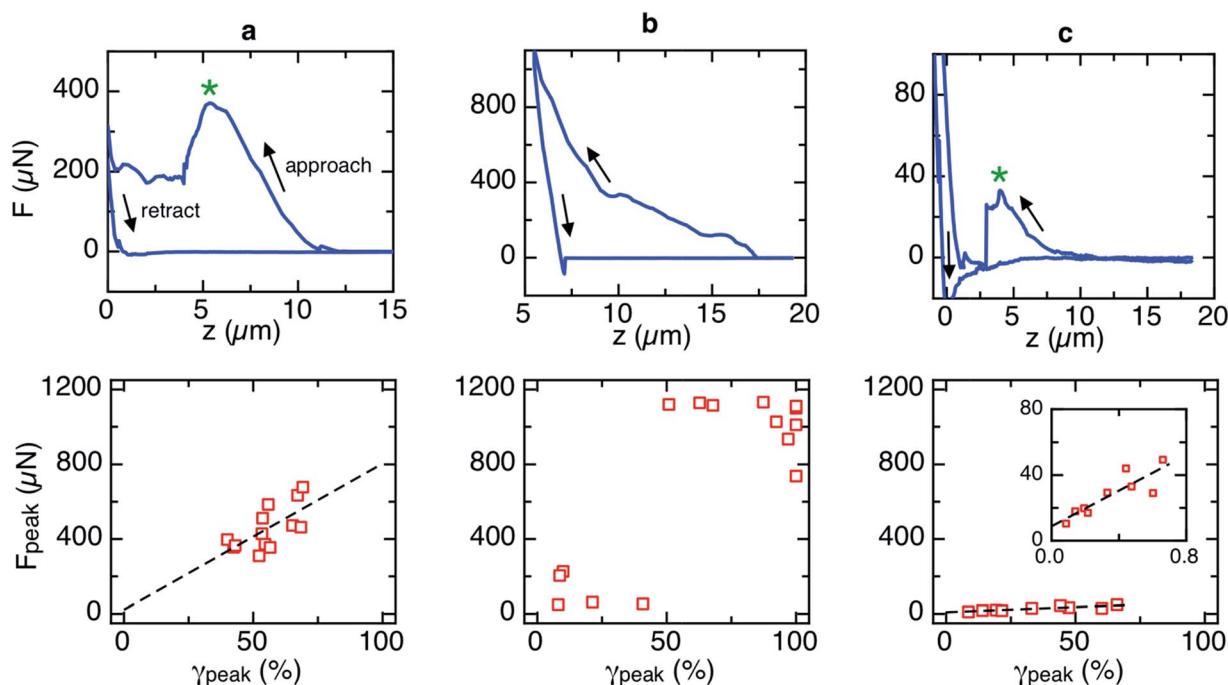
Fig. 11 Comparison of force–displacement curves of classical melamine/formaldehyde-based microcapsules (a) with two different formaldehyde-free microcapsules: crosslinked with guanazole in the aqueous phase (b), and HDI initially added to the oil phase (c). Top row: typical approach and retract force curves for each case (F: compressive force; z: displacement of the force probe; $z = 0$ μm: position of the glass substrate; star symbols indicate capsule rupture). Bottom row: peak force F_{peak} *vs.* deformation at rupture γ_{peak} from tests on multiple microcapsules; $\gamma_{peak} = 100\%$ corresponds to complete compression of the capsule). Dashed lines are linear curve fits to describe the relation between force and deformation at the rupture point. The inset in c shows a magnified portion of the main graph.

the force reached at peak value). These plots also identify three different rupture characteristics: the classical melamine/ formaldehyde capsules (case a in Fig. 11) rupture around a critical deformation in a rather narrow range around $\gamma_{peak} = 56\% \pm 8\%$, *i.e.* when compressed to about half their original diameter. Their corresponding peak forces are scattered in a relatively wide range of $F_{peak} \approx 310$–680 μN. In contrast, the formaldehyde-free capsules formed from HDI-containing oil drops (case c in Fig. 11) rupture at lower peak forces in a rather narrow range around $F_{peak} \approx 27 \pm 10$ μN, but their rupture occurs over a wider range of critical deformations $\gamma_{peak} \approx 9$– 66%. For both the classical melamine/formaldehyde capsules and the formaldehyde-free capsules formed from HDI-containing oil, the rupture force scales linearly with the deformation at rupture, *i.e.* $F_{peak} \propto \gamma_{peak}$. Interestingly, the correlation is defined better for the new formaldehyde free microcapsules (case c in Fig. 11 with $F_{peak} \approx (54 \text{ N})\gamma_{peak}$ and a correlation coefficient of 0.8655) than for the classical melamine/formaldehyde capsules (case a in Fig. 11 with $F_{peak} \approx (783 \text{ N})\gamma_{peak}$ and a correlation coefficient of 0.6650). For capsules crosslinked with amines in the aqueous phase (case b), no rupture occurs except for very few capsules, therefore, no meaningful correlation between peak force and deformation at the peak force could be found, as the force either reaches the maximum force achievable with the sensor used (around 1100 μN), or the capsule is compressed to completion without exhibiting a sudden rupture (*i.e.* γ_{peak} approaches 100%).

3. Conclusions

In this contribution, we presented a new approach to synthesize formaldehyde-free melamine microcapsules with controlled mechanical characteristics and with barrier properties suitable for the encapsulation of volatile compounds, and in particular for fragrance oils. This approach is based on the deposition of newly synthesized formaldehyde-free resins at the interface of oil droplets, in combination with *in situ* crosslinking to enhance the barrier properties. In particular, thanks to the use of LC/ESI-TOF-MS, it was possible to characterize and understand the mechanism of the polymerization between glyoxal and its derivatives and melamine, urea or guanazole to prepare various oligomers of formaldehyde-free aminoplast resin. We found that the combined synthesis of an optimized composition of aminoplast copolymers followed by *in situ* crosslinking using hexamethylenediisocyanate (HDI) yields stable and robust core/shell capsules with controlled mechanical properties. In contrast to classical melamine–formaldehyde microcapsules, the combination of the separate resin deposition and crosslinking steps also allows to develop microcapsules with more diverse mechanical properties than classical melamine capsules, therefore allowing the shell properties to be adapted to different application conditions. For example, the polymer shell material can be synthesized such that chemical stability and low permeability of the

microcapsules are achieved, yet they remain sufficiently breakable to easily release their encapsulated load under typical application conditions.

4. Experimental section

4.1. Raw materials

1,3,5-Triazine-2,4,6-triamine, urea, formic acid, hexamethylene diisocyanate, oxalaldehyde (aqueous solution at 40 wt%), and 2,2-dimethoxyacetaldehyde (aqueous solution at 60 wt%) were all supplied by Sigma-Aldrich Switzerland and used as received. Nitric acid and sodium hydroxide were used as an aqueous solution at 30 wt%. 1H-1,2,4-Triazole-3,5-diamine (guanazole) was purchased from Alfa Aesar. Alcapsol 144 was supplied by Ciba Specialty Chemicals Water Treatments Limited and used as an aqueous solution at 20 wt%. Ambergum 1221 (CAS 9004-32-4), M_w 35 000–50 000 g mol^{-1} with a degree of substitution of 1.2, was supplied by Ashland Inc and used as an aqueous solution at 2 wt%. Five different volatile molecules, methyl 2,2-dimethyl-6-methylene cyclohexane-1-carboxylate, 2-(*tert*-butyl) cyclohexyl acetate, 4-(*tert*-butyl)cyclohexyl acetate, 3-(4-(*tert*-butyl)phenyl)-2-methylpropanal and hexyl 2-hydroxybenzoate, were supplied by Firmenich SA, and used each at 20 wt% in the oil phase to prepare the emulsions (Table 10).

4.2. Liquid chromatography/electrospray ionization-time of flight-mass spectrometry (LC/ESI-TOF-MS) analyses

Analyses of the resins of amines and aldehydes were carried out in aqueous solution of formic acid at 0.1 wt% at RT on an Agilent 1200 HPLC system composed of a binary solvent manager (or pump G1312b), an auto sampler (g1329a), and an Agilent G1969A MS TOF system composed of a multimode source APCI + ESI. The standard mobile phase was a water premix of formic acid 0.1% (Biosolve no. 23244125 ULC/MSD lot 550361) eluted at 0.5 mL min^{-1}, injection volume: 1 µL with well plate sampler (without column), temperature of thermostat at 60 °C (±0.1 °C). One blank run was performed between each sample. The MS detector was a Multi-mode Electro spray (ESI) + APCI Pos LCMSD TOF with a high resolution at 3 ppm acq. The

source was a mode positive, charging voltage 2000 V, V cap 2500 V, Corona 4 µA, drying gas N$_2$, 5 L min^{-1} at 325 °C, nebuliser 30 psig at 200 °C, fragmentor from 140 to 320 V, m/z scan range from 103 to 3000, with online standard for mass adjustment (TOF high resolution > 10 000). Calculated results with an error <20 ppm were displayed.

4.3. Preparation of resins

4.3.1. Preparation of copolymer 3. In a round bottom flask of 100 mL, 1,3,5-triazine-2,4,6-triamine (11.20 g, 89 mmol) and 2,2-dimethoxyacetaldehyde (30.81 g, 178 mmol) were added. Water (3.69 g, 205 mmol) was added. The pH was adjusted to 9.41 with 0.27 g of sodium hydroxide (aq. solution at 30 wt%). The mixture was heated at 60 °C for 2 h. Then, nitric acid (30 wt% in water, 2.67 g) was added to give a pH of 4.49. The mixture was heated at 60 °C for 4 h to give a solution. The mixture was then stored at 3 °C in the fridge. An aliquot was introduced into an aqueous solution of formic acid (0.1 wt%) to be analyzed. The solid content was determined to be 58 wt% by TGA at 50 °C.

4.3.2. Preparation of copolymer 4

(4a, 4a′, 4c–e). In a 250 mL round-bottomed flask, oxalaldehyde (3.45 g, 23.8 mmol) was added in water (15 mL) to give a colorless solution (pH 3.55). 1,3,5-Triazine-2,4,6-triamine (2.01 g, 15.9 mmol) was added slowly and the pH was controlled to be between 4 and 5 during the addition of nitric acid. The reaction mixture was stirred for 0.1 to 2.5 h at 60 °C or 80 °C.

(4b). In a 250 mL round-bottomed flask oxalaldehyde (10.36 g, 71.4 mmol) was added in water (25 mL) to give a colorless solution. 1,3,5-Triazine-2,4,6-triamine (1.50 g, 11.89 mmol) was added slowly. Nitric acid was added to control the pH at 4.8. The reaction mixture was stirred at 60 °C for 1 h and then divided into two parts. One part was stirred at 90 °C for 2 h. The different reaction mixtures of copolymers **4** were slowly cooled to room temperature under stirring and kept at 3 °C in the fridge. An aliquot was introduced in formic acid 0.1 wt% aqueous solution to be analyzed.

4.3.3. Preparation of copolymer 6

(6a, 6c). In a 100 mL round-bottomed flask, urea (2.99 g, 49.9 mmol) and oxalaldehyde (7.25 g, 50.0 mmol) were mixed to give a colorless solution. A solution of sodium hydroxide was added to obtain a pH of 9.4. The reaction mixture was stirred at 60 °C for 30 min to give a colorless solution (pH 4.82). The medium was slowly cooled to room temperature under stirring and kept to fridge.

(6b, 6d). In a 250 mL round-bottomed flask urea (2.0045 g, 33,4 mmol) was dissolved in water (10 mL) to give a colorless suspension. Oxalaldehyde (4.83 g, 33.3 mmol) was added to the reaction mixture (pH 3.83). A solution of sodium hydroxide was added to obtain a pH of 6 and the reaction mixture was stirred at 60 °C for 3 h to give a colorless solution.

(6e–6h). In a 100 mL round-bottomed flask urea (3.00 g, 50.0 mmol) and a solution of oxalaldehyde (3.62 g, 24.98 mmol) was mixed together. A solution of sodium hydroxide was added to obtain a pH of 9.0. The reaction mixture was stirred at 60 °C for

Table 10 Structures of volatile bioactive molecules present at 20 wt% in the oil phase of the oil-in-water emulsion

Molecule	Structure
Methyl 2,2-dimethyl-6-methylene cyclohexane-1-carboxylate	
2-(*tert*-Butyl)cyclohexyl acetate	
(1*S*,4*S*) or (1*R*,4*R*)-4-(*tert*-butyl)cyclohexyl acetate	
3-(4-(*tert*-Butyl)phenyl)-2-methylpropanal	
Hexyl 2-hydroxybenzoate	

1 h. The pH was then adjusted to 4.6 with a solution of formic acid and the reaction was stirred at 80 °C for 1 h.

(6i). In a 100 mL round-bottomed flask urea (6.001 g, 100 mmol) and oxalaldehyde (3.69 g, 25.4 mmol) were mixed to give a colorless solution. The pH was adjusted with a solution of sodium hydroxide to 8.8. The reaction mixture was stirred at 80 °C for 30 min. The pH was adjusted with a solution of formic acid to 4.5 and the reaction mixture was stirred at 80 °C for 6 h. All reaction mixtures of copolymers **6** were slowly cooled to room temperature under stirring and kept at 3 °C in the fridge. Aliquots were introduced in an aqueous solution of formic acid (0.1 wt%) before analysis.

4.3.4. Preparation of copolymer 7.
In a 250 mL round-bottomed flask, 1*H*-1,2,4-triazole-3,5-diamine (1.90 g, 19.2 mmol) was dissolved in water (37 mL) to give a yellow solution. A solution of oxalaldehyde (1.11 g, 1.91 mmol) was then added (pH 7.98). The reaction mixture was stirred at 60 °C for 3.5 h. Samples were collected and cooled to room temperature, kept at 3 °C after reaction time of 20 min, 45 min, 1 h, 2.5 h and 3.5 h to be analyzed by LC/ESI-TOF-MS.

4.3.5. Preparation of copolymer 9

(9a). In a round bottom flask of 250 mL, 1,3,5-triazine-2,4,6-triamine (9.3 g, 74 mmol), urea (13.33 g, 222 mmol), 2,2-dimethoxyacetaldehyde (12.8 g, 74 mmol) and oxalaldehyde (42.9 g, 296 mmol) were dissolved in water (11 g, 611 mmol). The pH was adjusted with 1.3 g of sodium hydroxide (aq. solution at 30 wt%, pH 9.03). The mixture was heated at 60 °C for 20 min. Then, nitric acid (aq. solution at 30 wt%, 19.0 g) was added to adjust the pH to 4.48. The mixture was heated at 60 °C for 4 h. The solution was stored at 3 °C (pH = 4.57). The solid content was 49 wt% (measured by TGA).

(9b–9c). In a 250 mL round-bottomed flask oxalaldehyde (2.30 g, 15.87 mmol) was dissolved in water (4.5 mL). 1,3,5-Triazine-2,4,6-triamine (2.00 g, 15.87 mmol) was added slowly and the pH was adjusted to 4.55 with a solution of formic acid. The reaction mixture was stirred at 80 °C for 30 min. Urea (2.86 g, 47.7 mmol) was added and the pH was controlled to be at 5.5. The reaction mixture was stirred at 80 °C for 4 h (pH 5.35). Samples of copolymers **9** were collected and cooled to room temperature before analyses by LC/ESI-TOF-MS.

4.4. General procedure to prepare resins for microcapsules A–D

In a round-bottomed flask, solutions of oxalaldehyde and 2,2-dimethoxyacetaldehyde were dissolved in water. 1,3,5-Triazine-2,4,6-triamine and urea were added to the reaction mixture and the pH was adjusted to 9.0 with a solution of sodium hydroxide. The reaction mixture was stirred at 60 °C for 20 min. A solution of nitric acid was added to obtain a pH of 4.6 and the reaction mixture was stirred at 60 °C for 4 h. The reaction was stopped and cooled down to room temperature under stirring to give a yellow solution. The solid content was finally measured by TGA.

The resin for microcapsules **A9** was prepared with oxalaldehyde (10.40 g, 71.7 mmol), 2,2-dimethoxyacetaldehyde (6.20 g, 35.7 mmol), water (5 mL), 1,3,5-triazine-2,4,6-triamine (2.51 g,

19.9 mmol) and urea (3.57 g, 59.5 mmol). The solid content was 49.2 wt%. The resin for microcapsule **B9** was prepared with 1,3,5-triazine-2,4,6-triamine (9.33 g, 74 mmol), urea (13.33 g, 222 mmol), 2,2-dimethoxyacetaldehyde (12.84 g, 74 mmol) and oxalaldehyde (42.9 g, 296 mmol), water (11 mL). The solid content was 49.0 wt%. The resin for microcapsule **C9** was prepared with oxalaldehyde (14.37 g, 99.0 mmol), 2,2-dimethoxyacetaldehyde (2.86 g, 16.5 mmol), water (5.1 mL), 1,3,5-triazine-2,4,6-triamine (3.00 g, 23.8 mmol) and urea (4.29 g, 71.5 mmol). The solid content was 46.7 wt%. The resin in capsules **D9** was prepared with 2,2-dimethoxyacetaldehyde (1.76 g, 10.2 mmol), oxalaldehyde (14.86 g, 102.0 mmol), water (4.5 mL), 1,3,5-triazine-2,4,6-triamine (3.02 g, 23.9 mmol) and urea (4.30 g, 71.5 mmol). The solid content was 45.8 wt%.

4.5. General procedure to prepare cross-linked microcapsule B

In a Schmizo reactor (200 mL), an aqueous solution of Ambergum 1221 (15.0 g, 0.43 wt% in the capsule dispersion) and a solution of resin (see **B9**, 4.5 g, from 2.95 to 3.15 wt% in the capsule dispersion) were added into water (30 mL). The reaction mixture was stirred for 30 min at RT (pH between 4.8 and 5.3). A solution of volatile compounds (20 g, 28.5 wt% of the capsule dispersion) was added to the reaction mixture and emulsified with an ultra turrax at 24 000 rpm at RT for 2 min. An aqueous solution of Alcapsol 144 (0.4 g, 0.11 wt% of the capsule dispersion) was added to the emulsion, which was then stirred at 300 rpm with an anchor-shaped paddle at 40 °C for 1 h, and then at 60 °C for 1 h to give a white dispersion.

4.5.1. Cross-linking of the capsule B from the aqueous phase.
A solution of urea (capsules **B-U**) or guanazole (capsules **B-GZ**) was added to the dispersion of capsules **B**, which was stirred at 60 °C for 1 h, and finally at 75 °C for 3 h. The capsule dispersions **B-U** and **B-GZ** were neutralized with a solution of sodium hydroxide and stored at room temperature.

4.5.2. Cross-linking of the capsule B from the oil phase.
Capsules **B-H** were prepared according to the protocol of capsule **B** with a solution of hexamethylenediisocyanate **10** at various concentrations in the mixture of volatile molecules.

4.6. Interfacial tension

The interfacial tensions of resins **A9–D9** solutions at 3 wt% in water with the model perfume were measured by the pendant drop method with a Drop Shape Analysis System DSA 10 Mk2 (Krüss, Germany) and a high-speed video measuring system (PA3030, 360 pictures per second) for automatic contact angle and surface tension measurement. A frame grabber and a 6-fold zoom lens have been brought to the camera. Drops of the polymer aqueous solution in perfume oil were formed using a syringe with a diameter of 1.8 mm; the syringe diameter was used to calculate the magnification factor and then the volume of the drop.

4.7. Thermogravimetric analysis

Solid content, volatile retention and thermal stability were assessed by using a thermogravimetric analyzer (TGA/

SDTA851e, Mettler-Toledo, Switzerland) equipped with a microbalance having an accuracy of 1 μg and a 35 mL oven. The sample (circa 12 mg) was introduced into an aluminium oxide crucible (70 μL) and its mass was measured as a function of the temperature and the time under a constant flow of nitrogen (20 mL min^{-1}). The solid content and the perfume retention of the sample was measured at temperatures from 25 °C to 50 °C at a rate of 5 °C min^{-1} and then at 50 °C for four hours.

4.8. Size distribution

The size distribution of the microcapsule suspensions were measured and analyzed by flow particle imaging using the Sysmex FPIA-3000 (Malvern Instruments, UK). This method allowed the characterization of the particle size distribution as well as particle shape distributions using automated imaging techniques.

4.9. Force measurements on microcapsules

Force-displacement curves on single microcapsules were measured with a micromechanical testing device (FT-FS1000, FemtoTools, Switzerland). The microcapsules were diluted in Millipore® water, deposited on microscope cover slides, and dried under low vacuum during 10 min. A custom-built inverse microscope was used to image the capsules on the glass slide, and a second lateral microscope was used to view the vertical position of the force probe. The zero position for the displacement values was detected with the force sensor positioned on a free spot on the glass substrate. Approach and retract curves, starting at a distance of 20.0 μm from the surface of the glass substrate, were measured for several individual capsules of each sample at a constant absolute speed of 0.5 μm s^{-1}. The tip of the force sensor has flat surface oriented in parallel to the glass substrate, *i.e.* the experiments amount to a controlled-speed compression of the capsules between two flat surfaces.

References

1 S.-J. Park and R. Arshady, *Microspheres, Microcapsules Liposomes*, 2003, **6**, 157–198.

2 A. L. Becker, A. P. R. Johnston and F. Caruso, *Small*, 2010, **6**, 1836–1852.

3 J. Zhao, C. Allen and A. Eisenberg, *Macromolecules*, 1997, **30**, 7143–7150.

4 K. Kataoka, G. S. Kwon, M. Yokoyama, T. Okano and Y. Sakurai, *J. Controlled Release*, 1993, **24**, 119–132.

5 D. L. Berthier, I. Schmidt, W. Fieber, C. Schatz, A. Furrer, K. Wong and S. Lecommandoux, *Langmuir*, 2010, **26**(11), 7953–7961.

6 A. Herrmann, *Angew. Chem.*, 2007, **119**, 5909; *Angew. Chem., Int. Ed.*, 2007, **46**, 5836–5863.

7 S. Bône, C. Vautrin, V. Barbesant, S. Truchon, I. Harrison and C. Geffroy, *Chimia*, 2011, **65**(3), 177–181.

8 J. Ness, O. Simonsen and K. Symes, *Microspheres, Microcapsules Liposomes*, 2003, **6**, 199–234.

9 H. N. Yow and A. F. Routh, *Soft Matter*, 2006, **2**, 940–949.

10 A. P. Esser-Kahn, S. A. Odom, N. R. Sottos, S. R. White and J. S. Moore, *Macromolecules*, 2011, **44**, 5539–5553.

11 P. W. Chen, R. M. Erb and A. R. Studart, *Langmuir*, 2011, **28**, 144–152.

12 G. Sun and Z. Zhang, *J. Microencapsulation*, 2001, **18**(5), 593–602.

13 H. Y. Lee, S. J. Lee, I. W. Cheong and J. H. Kim, *J. Microencapsulation*, 2002, **19**(5), 559–569.

14 Y. He, J. Bowen, J. W. Andrews, M. Liu, J. Smets and Z. Zhang, *J. Microencapsulation*, 2014, **31**(5), 430–439.

15 T. Vöpel, R. Scholz, L. Davico, M. Groß, S. Büning, S. Kareth, E. Weidner and S. Ebbinghaus, *Chem. Commun.*, 2015, **51**, 6913–6916.

16 Q. Yi and G. B. Sukhorukov, *Soft Matter*, 2014, **10**, 1384–1391.

17 N. Paret, A. Trachsel, D. L. Berthier and A. Herrmann, *Angew. Chem., Int. Ed.*, 2015, **54**, 2275–2279.

18 X. Q. Song, Y. X. Li and J. W. Wang, *Adv. Mater. Res.*, 2013, **815**, 367–370.

19 D. Blythe, D. Churchill, K. Glanz and J. Stutz, *Microspheres, Microcapsules Liposomes*, 1999, **1**, 419–439.

20 K. S. Lee, M. Rodson and H. B. Scher, *Pestic. Sci.*, 1998, **4**, 394–400.

21 M. Pretzl, M. Neubauer, M. Tekaat, C. Kunert, C. Kuttner, G. Leon, D. Berthier, P. Erni, L. Ouali and A. Fery, *ACS Appl. Mater. Interfaces*, 2012, **4**(6), 2940–2948.

22 R. Mercade-Prieto, R. Allen, D. York, J. A. Preece, T. E. Goodwin and Z. Zhang, *J. Microencapsulation*, 2012, **29**(5), 463–474.

23 P. Persico, C. Carfagna, L. Danicher and Y. Frere, *J. Microencapsulation*, 2005, **22**(5), 471–486.

24 H. Yoshizawa, E. Kamio, N. Hirabayashi, J. Jacobson and Y. Kitamura, *J. Microencapsulation*, 2004, **21**(3), 241–249.

25 K. Hong and S. Park, *J. Appl. Polym. Sci.*, 2000, **78**(4), 894–898.

26 J. Li, A. P. Hitchcock, H. D. H. Stöver and I. A Shirley, *Macromolecules*, 2009, **42**, 2428–2432.

27 K. Dietrich, E. Bonatz, H. Geistlinger, H. Herma, R. Nastke, H.-J. Purz, M. Schlawne and W. Teige, *Acta Polym.*, 1989, **40**(5), 325–331.

28 K. Dietrich, E. Bonatz, R. Nastke, H. Herma, M. Walter and W. Teige, *Acta Polym.*, 1990, **41**(2), 91–95.

29 C. Quellet and J. Hotz, Givaudan, CH2009000052, 2009.

30 P.-L. Lam, K. K.-H. Lee, S. H.-L. Kok, G. Y.-M. Cheng, X.-M. Tao, D. K.-P. Hau, M. C.-W. Yuen, K.-H. Lam, R. Gambari, C.-H. Chui and R. S.-M. Wong, *Soft Matter*, 2012, **8**, 5027–5037.

31 D. McGregor, A. Boobis, M. Binaglia, P. Botham, L. Hoffstadt, S. Hubbard, T. Petry, A. Riley, D. Schwartz and C. Hennes, *Crit. Rev. Toxicol.*, 2010, **40**(3), 245–285.

32 H. D. A. Heck, M. Casanova-Schmitz, P. B. Dodd, E. N. Schachter, T. J. Witek and T. Tosun, *Am. Ind. Hyg. Assoc. J.*, 1985, **46**(1), 1–3.

33 S. Norliana, A. S. Abdulamir, F. Abu Bakar and A. B. Salleh, *Am. J. Pharmacol. Toxicol.*, 2009, **4**(3), 98–106.

34 D. Berthier, G. Leon and N. Paret, Firmenich SA, IB2011052700, 2011.

35 D. Berthier, G. Leon, L. Ouali and N. Paret, Firmenich SA, EP2012071340, 2013.

36 W. Li, J. Wang, X. Wang, S. Wu and X. Zhang, *Colloid Polym. Sci.*, 2007, **285**(15), 1691–1697.

37 C. Tomasino and M. B. Taylor II, *Text. Chem. Color.*, 1984, **16**(12), 33–38.

38 Y. Long, D. York, Z. Zhang and J. A. Preece, *J. Mater. Chem.*, 2009, **19**(37), 6882–6887.

39 A. Despres, A. Pizzi, C. Vu and H. Pasch, *J. Appl. Polym. Sci.*, 2008, **110**(6), 3908–3916.

40 A. Despres, A. Pizzi, C. Vu and L. Delmotte, *Eur. J. Wood Wood Prod.*, 2010, **68**(1), 13–20.

41 O. Steinhof, É. J. Kibrik, G. Scherr and H. Hasse, *Magn. Reson. Chem.*, 2014, **52**(4), 138–162.

42 S. Lavric, D. Kocar, I. Mihelic and C. Braybrook, *Prog. Org. Coat.*, 2015, **81**, 27–34.

43 M. G. Voronkov, T. V. Kashik, V. V. Makarskii, V. A. Lopyrev, S. M. Ponomareva and E. F. Shibanova, *Dokl. Akad. Nauk SSSR*, 1976, **227**(5), 1116–1119.

44 N. Bodor, M. J. S. Dewar and A. J. Harget, *J. Am. Chem. Soc.*, 1970, **92**(10), 2929–2936.

45 B. Andrade, Z. Song, J. Li, S. C. Zimmerman, J. Cheng, J. S. Moore, K. Harris and J. S. Katz, *ACS Appl. Mater. Interfaces*, 2015, **7**, 6359–6368.